Interstitial cells of Cajal in the deep muscular plexus mediate enteric motor neurotransmission in the mouse small intestine

Sean M. Ward, Gerald J. McLaren and Kenton M. Sanders

Department of Physiology and Cell Biology, University of Nevada School of Medicine, Reno, NV 89557, USA

Interstitial cells of Cajal (ICC) provide important regulatory functions in the motor activity of the gastrointestinal tract. In the small intestine, ICC in the myenteric region (ICC-MY), between the circular and longitudinal muscle layers, generate and propagate electrical slow waves. Another population of ICC lies in the plane of the deep muscular plexus (ICC-DMP), and these cells are closely associated with varicose nerve terminals of enteric motor neurons. Here we tested the hypothesis that ICC-DMP mediate excitatory and inhibitory neural inputs in the small bowel. ICC-DMP develop largely after birth. ICC-DMP, with receptor tyrosine kinase Kit-like immunoreactivity, appear first in the jejunum and then in the ileum. We performed electrophysiological experiments on mice immediately after birth (P0) or at 10 days post partum (P10) to determine whether neural responses follow development of ICC-DMP. At P0, slow-wave activity was present in the jejunum, but neural responses were poorly developed. By P10, after ICC-DMP developed, both cholinergic excitatory and nitrergic inhibitory neural responses were intact. Muscles of P0 mice were also put into organotypic cultures and treated with a neutralizing Kit antibody. Neural responses developed in culture within 3–6 days in control muscles, but blocking Kit caused loss of ICC and loss of cholinergic and nitrergic neural responses. Non-cholinergic excitatory responses remained after loss of ICC-DMP. Our observations are consistent with the idea that cholinergic and nitrergic motor neural inputs are mediated, to a large extent, via ICC-DMP. Thus, ICC-DMP appear to serve a function in the small intestine that is similar to the role of the intramuscular ICC in the stomach.

(Resubmitted 11 January 2006; accepted after revision 27 February 2006; first published online 2 March 2006)
Corresponding author K. M. Sanders: Department of Physiology and Cell Biology, University of Nevada School of Medicine, Reno, NV 89557, USA. Email: kent@unr.edu

Interstitial cells of Cajal (ICC) serve important regulatory functions in gastrointestinal (GI) motility (e.g. Sanders, 1996). ICC can be grouped into different morphological and functional classes, and the different types of ICC participate in different aspects of motility regulation. ICC of the myenteric plexus region (ICC-MY) of the stomach, small intestine and colon and ICC along the submucosal surface of the circular muscle layer (ICC-SM) of the colon in some species are pacemaker cells that generate electrical slow waves (e.g. Langton *et al.* 1989; Ward *et al.* 1994; Huizinga *et al.* 1995; Torihashi *et al.* 1995; Dickens *et al.* 1999; Ordog *et al.* 2000). Intramuscular ICC (ICC-IM), found among the muscle fibres of the stomach and sphincteric regions, are involved in the mediation or modulation of enteric neurotransmission (Burns *et al.* 1996; Ward *et al.* 1998, 2000; Beckett *et al.* 2003; Suzuki *et al.* 2003). ICC-IM also influence electrical rhythmicity by transducing chronotropic signals from stretch and neural inputs (Beckett *et al.* 2003; Suzuki *et al.* 2003; Won *et al.* 2005).

ICC express the receptor tyrosine kinase, Kit, (Ward *et al.* 1994; Torihashi *et al.* 1995; Huizinga *et al.* 1995) and depend upon the Kit signalling pathway for development and maintenance of the ICC phenotype (Torihashi *et al.* 1995, 1997). Animals with mutations in *c-kit* and *steel*, which encodes stem cell factor, the ligand for Kit, have proven useful in determining the physiological functions of ICC. W/W^V mutants, a non-lethal compound heterozygote, have been most frequently used for studies of this type. The W mutation is a total ablation of the tyrosine kinase portion of c-*kit*, whereas W^V is a point mutation at AA660 rendering the tyrosine kinase less active, but still functional (Nocka *et al.* 1990). Only certain classes of ICC are lost in W/W^V mutants. ICC of the deep muscular plexus in the intestine (ICC-DMP), ICC-MY of the stomach (Burns *et al.* 1996; Hirst *et al.* 2002), and ICC

 DOI: 10.1113/jphysiol.2006.105189

in the colon (S. M. Ward and K. M. Sanders, unpublished observations) persist in W/W^V mutant animals. Studies using neutralizing antibodies to Kit have shown that all ICC are lost in the small bowel and colon when Kit is blocked (Torihashi *et al.* 1995). Thus, Kit is essential for the development of ICC, but there is variability in the degree of resistance that some ICC display to partial loss-of-function mutations (see Burns *et al.* 1996).

In the small intestine, ICC outside the myenteric region are concentrated in the region of the deep muscular plexus, and these cells have been referred to as ICC-DMP. As already mentioned, the network of ICC-DMP is not affected in W/W^V mice and to date there have been no clear means to determine the importance of these cells in small intestinal function. It would appear that ICC-DMP are not able to generate pacemaker activity in the mouse, because small intestines of W/W^V and *steel* (i.e. Sl/Sl^d) mutants contain ICC-DMP but lack slow waves (Ward *et al.* 1994). ICC-DMP are in close association with varicose nerve terminals in the DMP in humans and animal models (e.g. Lavin *et al.* 1998; Wang *et al.* 1999, 2003*b*; Iino *et al.* 2004), and it is possible that ICC-DMP, like ICC-IM in the stomach, are involved in mediating neurotransmission from enteric motor neurons.

We have shown previously that ICC-DMP networks develop after birth (Torihashi *et al.* 1997). It has been shown that differentiated enteric motor neurons (i.e. cholinergic and nitrergic) are present in the GI tract at birth (Young *et al.* 2002). In the present study, we tested whether the development of enteric motor neurotransmission follows the development of ICC-DMP. We have also found that apparently normal ICC networks develop in organotypic cultures removed from animals at birth (Ward *et al.* 1997), and here we have made use of small intestinal cultures to determine whether loss of ICC caused by blocking the Kit signalling pathway with neutralizing antibodies affects the development of enteric motor neurotransmission.

Methods

Animals

BALB/c mice, either newly born (P0) or at 10 days post partum (P10), were killed by anaesthetic inhalation with isoflurane (Baxter, Deerfield, IL, USA) and exsanguinated by cervical dislocation followed by decapitation. The use and treatment of animals was approved by the Institutional Animal Use and Care Committee at the University of Nevada.

Organ culture

Segments of jejunum were isolated from animals within 24 h after birth (approximately 50% of the animals had not suckled). The jejunal segments were opened along the mesenteric border, luminal contents were removed by flushing with Krebs–Ringer buffer (KRB) and the mucosa was removed by sharp dissection. Strips of muscle (5 mm × 2 mm) were cut and pinned to the base of a sterile tissue culture dish lined with Sylgard elastomer (Dow Corning Corp., Midland, MI, USA) with the mucosal side of the circular muscle facing upwards. Tissues were washed four times with KRB containing penicillin (200 U ml^{-1}), streptomycin (200 mg ml^{-1}) and amphotericin B (0.5 mg ml^{-1}) and placed in M199 medium (Sigma) containing similar concentrations of antibiotics and antimycotic. The muscles were incubated at 37°C (90% humidity and 95% O_2–5% CO_2) for 7–10 days, and the culture medium was changed every second day. Some tissues were incubated in M199 medium containing a neutralizing, anti-Kit antibody (ACK2; 5 μg ml^{-1}; see Maeda *et al.* 1992). Control muscle strips were prepared in the same manner from the same animals, but ACK2 was not added to the medium of control strips. Other control experiments were performed in which rat non-immune serum (5 μg ml^{-1}; Hyclone, Logan, UT, USA) was included in the incubation medium to control for possible non-specific side effects of antibody treatment.

Electrophysiological studies

For studies on fresh muscles, segments of jejunum were isolated from animals at P0 and P10 post partum. The jejunal segments were opened along the mesenteric border. Luminal contents were removed with KRB. After removing the mucosa, tissues (10 mm × 4 mm) were cut and pinned to the Sylgard elastomer floor of a recording chamber with the mucosal side of the circular muscle facing upwards. Cultured muscle strips were removed from the incubator and placed in the recording chamber after 7–10 days of culturing.

With both fresh tissues and cultured muscles, parallel platinum electrodes were placed on either side of the muscle strips to facilitate electrical field stimulation (EFS) via a square-wave pulse generator (Grass S48; Astro-Medical Industrial Park, West Warwick, RI, USA). Neural responses were elicited by pulses of EFS (1–20 Hz for 1 s, 0.5 ms in duration at supramaximal voltage determined by increasing stimulus until a maximal response was reached).

Circular muscle cells were impaled with glass microelectrodes filled with 3 M KCl (resistance, 50–80 MΩ). Transmembrane potentials were measured using a high-input impedance amplifier (WPI S-7071; Sarasota, FL, USA) and outputs displayed on a Tektronix 2430 digital oscilloscope. Electrical signals were recorded on magnetic tape (Racal 40S). Electrical recordings were made in the presence of nifedipine (2 μM) to reduce muscle

contraction. Atropine (1 μM) and N^{ω}-nitro-L-arginine (L-NNA; 200 μM) were used where stated to isolate muscarinic and nitrergic components of the nerve-evoked responses. These drugs were introduced into the perfusing solution and allowed to equilibrate for at least 15 min.

Immunohistochemistry

For examination of the distribution of ICC in freshly isolated tissues from P0 and P10 animals, the tunica muscularis was pinned to the Sylgard floor of a dissecting dish and stretched to 110% of the resting length and width before being fixed with acetone for 10 min at 4°C. After fixation, the muscle strips were removed from the Sylgard dish and washed with 0.01 M phosphate buffered saline (PBS, pH 7.4) with 0.3% Triton X-100 and incubated in the presence of bovine serum albumin (BSA, 1% for 1 h) to reduce non-specific binding. Tissues were then incubated with an antibody raised against Kit protein (ACK2, rat monoclonal antiserum, 5 μg ml^{-1}, Gibco BRL, Gaithersburg, MD, USA) overnight, washed in PBS and incubated in secondary antibody for 1 h at room temperature (21-22°C). To examine the distribution of ICC following periods of organ culture, tissues were stretched and fixed in the organ culture dish and processed in a manner similar to that described above.

Similar immunohistochemical procedures were performed on whole mounts to examine the number and distribution of enteric nerves within jejunal muscles from P0 and P10 animals. Rabbit anti-protein gene product 9.5 (PGP 9.5; 1 : 1000; Ultraclone Ltd, Isle of Wight; UK), sheep anti-neuronal nitric oxide synthase (nNOS; 1 : 1000; gift from Piers Emson, Molecular Science Group, Cambridge, UK) and goat anti-vesicular acetylcholine transporter (vACh-T; 1 : 200; Chemicon International Inc., Temecula, CA, USA) were used to examine the presence and distributions of inhibitory nitrergic and excitatory cholinergic neurons. P0 tissues, organ cultured for 10 days with and without ACK2, were also examined with anti-neural antibodies. For secondary antibody labelling, Alexa fluor 488 coupled to chicken anti-rabbit, donkey anti-sheep or donkey anti-goat IgG antibodies (Molecular Probes, Eugene, OR, USA) were used at a dilution of 1 : 500 in PBS.

Cryostat sections

For examination of Kit labelling on cryostat sections of intact small intestines from P0 and P10 animals, intestines were flushed with PBS to remove luminal contents and immediately fixed in acetone (4°C for 10 min). Tissues were subsequently washed with PBS (four times for 15 min each), dehydrated in graded sucrose solutions (5–25% in PBS), embedded in Tissue Tek (optimal cutting temperature (O.T.C.)) compound (Sakura Finetek, Torrance, CA, USA) and frozen in isopentane precooled in liquid nitrogen. Sections were cut parallel and transverse to the circular muscle at a thickness of 10 μm using a Leica CM 3050 cryostat (Leica Microsystems, Wetzlar, Germany) and collected on slides treated with Vectabond (Vector Laboratories, Burlingame, CA, USA). For organ cultures, tissues were fixed in acetone after 7–10 days of culturing, dehydrated in sucrose and frozen as described above. Sections were preincubated with a solution of 1.0% BSA and 0.03% Triton X-100 made up in 0.1 M PBS for 1 h before incubation with primary antibody. After tissues were incubated with primary antibody, they were washed with PBS for at least 1 h, before incubation in secondary antibody for 1 h at room temperature. For secondary antibody labelling, Alexa fluor 594-coupled goat anti-rat IgG (Molecular Probes) was used. Secondary antibody was diluted to 1 : 200 in PBS. After washing with PBS, specimens were mounted with Vectashield (Vector Laboratories). Control tissues were prepared by either omitting primary or secondary antibodies from the incubation solutions.

Tissues were examined with a Biorad MRC 600 (Hercules, CA, USA) or a Zeiss LSM 510 Meta confocal microscope (Zeiss, Germany) with an excitation wavelength of 568 nm. Confocal micrographs shown are digital composites of *Z*-series scans of several optical sections (5–40 μm) through a depth of full or partial thickness of musculature. Final images were constructed with Bio-Rad Comos or Zeiss LSM 5 Image Examiner and Adobe Photoshop 7 software (Adobe Systems Inc., San Jose, CA, USA).

Solutions and drugs

The bath chambers was constantly perfused with oxygenated KRB containing (mM): NaCl 118.5, KCl 4.5, $MgCl_2$ 1.2, $NaHCO_3$ 23.8, KH_2PO_4 1.2, dextrose 11.0 and

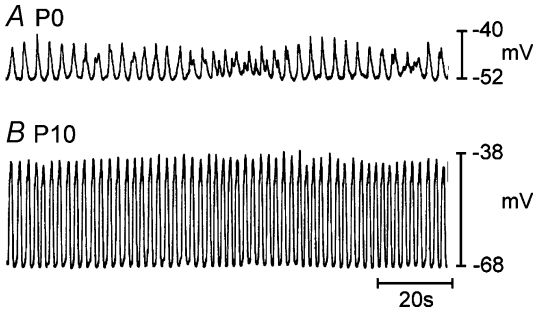

Figure 1. Development of electrical rhythmicity in the murine jejunum
A, shows typical electrical activity recorded from the circular muscle layer of the jejunum from a P0 animal. Jejunal tissues from P0 animals had irregular activity with slow waves that increased and decreased in amplitude. *B*, shows activity recorded from a P10 animal. Membrane potential and frequency and amplitude of slow waves increased within the first 10 days after birth.

$CaCl_2$ 2.4. The pH of the KRB was 7.3–7.4 when bubbled with 97% O_2–3% CO_2 at 37 ± 0.5°C. Muscles were left to equilibrate for at least 1 h before experiments were begun. For electrophysiological experiments, nifedipine was obtained from Sigma (St Louis, MO, USA) and dissolved in ethanol at a stock concentration of 10 mM before being added to the perfusion solution at a final concentration of 1 μM. Atropine, and L-NNA were also obtained from Sigma and dissolved in de-ionized H_2O before being diluted in KRB to the final concentration as stated in the Results.

Data analysis

Data are expressed as means ± S.E.M. Student's *t* test was used where appropriate to evaluate differences in the data. *P* values less than 0.05 were taken as a statistically significant difference. *P* values were obtained by averaging the number of cellular recordings from each tissue and then averaging the mean number from each muscle strip. The *n* values reported in the text refer to the number of muscle strips used for each experimental protocol. Each muscle strip was taken from a separate animal. Several electrical

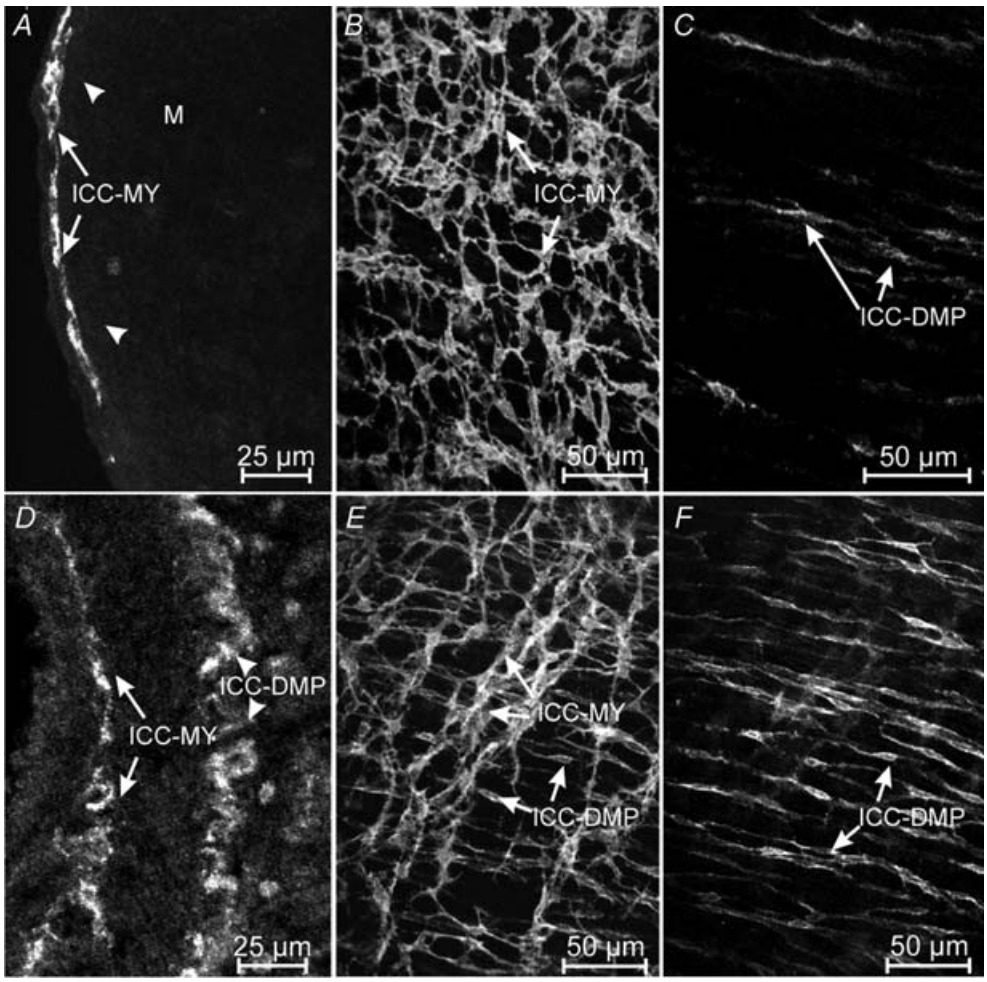

Figure 2. Development of Kit-expressing ICC-DMP in the murine jejunum
A–C, show the density and distribution of ICC in a P0 animal. *A*, is a cryostat section revealing ICC at the level of the myenteric plexus (ICC-MY, arrows). ICC at the deep muscular plexus (arrow heads) were not readily observed in cryostat sections. *B*, is a digital reconstruction from confocal images of a whole-mount preparation of the murine jejunum. ICC-MY form a distinct network (arrows) at P0 but ICC-DMP were few. *C*, is a digital reconstruction of the DMP of the whole mount in *B*. Occasional ICC-DMP (arrows) were observed, but they did not form a distinct network. *D–F*, reveal the density and distribution of ICC in the jejunum of a P10 animal. *D*, is a cryostat section showing ICC at the myenteric (ICC-MY) and deep muscular plexuses (ICC-DMP). *E*, is a confocal image of a whole-mount preparation of the jejunum from a P10 animal revealing ICC at the myenteric (ICC-MY) and deep muscular plexuses (ICC-DMP). *F*, is a digital reconstruction of the level of the deep muscular plexus of the same whole mount as in *E*. ICC-DMP (arrows) are more dense than at P0 and form a network by P10. Scale bar is indicated in each panel.

parameters were analysed: (i) resting membrane potential (RMP); (ii) slow-wave amplitude; and (iii) slow-wave frequency. Figures displayed were made from digitized data using Adobe Photoshop 7.0 and Corel Draw 7.0 (Corel Corp., Ontario, Canada).

Results

Development of spontaneous electrical activity

Circular muscles of the jejunum displayed rhythmic electrical activity (slow waves) at birth. The mean resting membrane potential (most negative potential between slow waves) on P0 was -58 ± 1 mV ($n = 11$). Slow waves averaged 11 ± 1 mV in amplitude, but were variable in amplitude from event to event in a given muscle strip. The average frequency of slow waves in these muscles was 17.6 ± 0.5 cycles min^{-1} (Fig. 1*A*). Resting membrane potential became more negative and slow waves increased in amplitude and became more regular during the first week after birth, as previously reported (Ward *et al.* 1997). By P10, resting membrane potential was significantly more negative than on P0 and averaged -66 ± 1 mV ($n = 6$, $P < 0.01$). Slow waves increased in amplitude (to 27 ± 1 mV; $n = 22$, $P < 0.01$) and frequency (to 26.8 ± 1.2 cycles min^{-1}; $n = 22$, $P < 0.01$) by P10 (Fig. 1*B*). Activity recorded by P10 was similar to that observed in adult tissues (see Ward *et al.* 1994).

Development of neuromuscular regulation in the small intestine

At the time of birth, ICC in the myenteric plexus region (ICC-MY) of the jejunum were intensely labelled with an antibody for Kit (ACK2; Fig. 2*A*). Whole mounts revealed that ICC-MY formed a dense network (Fig. 2*B*) similar to the distribution of these cells in adult tissues (Ward *et al.* 1997). ICC in the deep muscular plexus (ICC-DMP) were difficult to identify in cryostat cross-sections, but a few of these cells could be visualized in whole-mount preparations (Fig. 2*C*). At this stage of development, Kit-positive cells in the DMP were isolated from each other and showed no evidence of forming a network. In tissues removed from animals at P10, Kit-positive cells were abundant at two levels (Fig. 2*D*), and whole mounts revealed typical networks of ICC-MY and ICC-DMP (Fig. 2*E* and *F*), as previously described (Torihashi *et al.* 1995; Ward *et al.* 1995, 1997; Iino *et al.* 2004). These observations demonstrate the dramatic expansion in the Kit-positive cell population at the level of the DMP and organization of these cells into networks typical of adult tissues (Iino *et al.* 2004) within the first 10 days after birth. ICC-DMP in adult tissues are closely associated with enteric motor neurons (Lavin *et al.* 1998; Wang *et al.* 1999; Iino *et al.* 2004). Thus, we characterized the development of post-junctional neural responses in intestinal tissues between P0 and P10.

Neural responses in P0 muscles were small in amplitude and superimposed upon slow waves of varying amplitude, making distinctive, nerve-evoked responses difficult to resolve. Under control conditions, EFS of intrinsic nerves resulted in frequency-dependent depolarization that followed the stimulus ('off response'). Slow waves were superimposed upon the off responses (Fig. 3*A*). Atropine (1 μM) slightly reduced the off response caused by EFS, but the reduction did not reach significance at the lower frequencies of stimulation (1–10 Hz). Atropine failed to unmask inhibitory responses in all but one tissue (Fig. 3*B*). L-NNA (200 μM) had no significant effect on

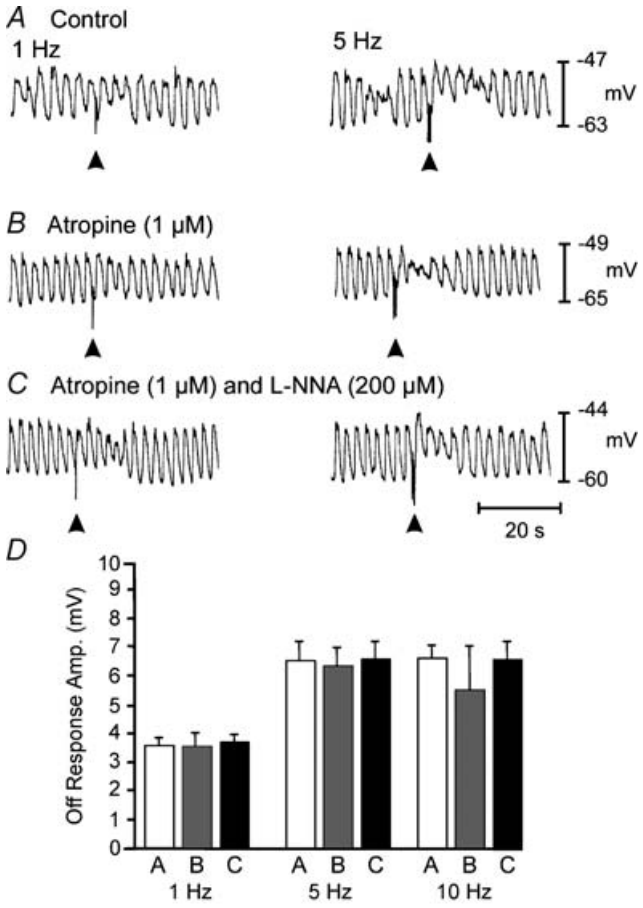

Figure 3. Neural responses recorded from the jejunum of a P0 animal

Responses to electric EFS (1- and 5-Hz trains for 1 s, pulse duration, 0.5 ms). EFS was delivered at the arrow heads in each trace. Under control conditions, neural responses consisted of a frequency-dependent off response with slow waves superimposed. Atropine (1 μM; *B*) alone or in the presence of L-NNA (200 μM; *C*) had little effect. *D*, summarizes the amplitudes of the off responses under control conditions (open bar) in the presence of atropine (grey bar) and in the presence of atropine plus L-NNA (filled bar) at 1, 5 and 10 Hz, respectively.

the magnitude of the excitatory responses in muscles of six of the seven animals (Fig. 3*C*). In one animal, atropine unmasked a small inhibitory response and this response was blocked by L-NNA (data not shown). The off responses in P0 animals are summarized in Fig. 3*D*.

EFS caused more robust responses in muscles of P10 animals. These responses were characterized by distinct inhibitory junction potentials (IJPs) and attenuation of slow waves for one or more cycles (Fig. 4*A*). At 1 Hz, the amplitude of the IJPs was 4.0 ± 0.7 mV ($n = 7$), and the amplitude increased to 5.2 ± 1.4 mV at 5 Hz ($n = 5$). Higher frequencies (> 5 Hz; data not shown) did not enhance the amplitudes of IJPs. Atropine (1 μM; Fig. 4*B*) had no significant effect on the amplitude of IJPs, but slow waves were further reduced in amplitude for several cycles following EFS. L-NNA (200 μM), in the presence of atropine (1 μM), significantly reduced the amplitudes of IJPs ($P < 0.05$ for frequencies of 1–5 Hz; Fig. 4*B* and *C*) and reduced the attenuation in slow-wave amplitude following EFS. Neural responses in P10 animals are summarized in Fig. 4*D* and *E*.

Our data suggest that development of ICC-DMP may initiate cholinergic and nitrergic neuromuscular regulation in the small intestine. Another explanation might be that enteric neurons are not fully developed at birth, and the delays in development of cholinergic and nitrergic responses could be due to post-natal maturation of these neural pathways. To test this possibility, whole-mount preparations of P0 and P10 jejunal muscles were labelled with antibodies against the pan neuronal marker PGP 9.5, and vAChT and nNOS (as markers for excitatory and inhibitory motor neurons, respectively). At P0, PGP 9.5-like immunopositive neurons were organized into myenteric ganglia and varicose processes were distributed within the deep muscular plexus of the circular muscle layer (Fig. 5*A*). Neurons with vAChT-like and nNOS-like immunoreactivity innervated the circular muscle (Fig. 5*B* and *C*, respectively). At P10,

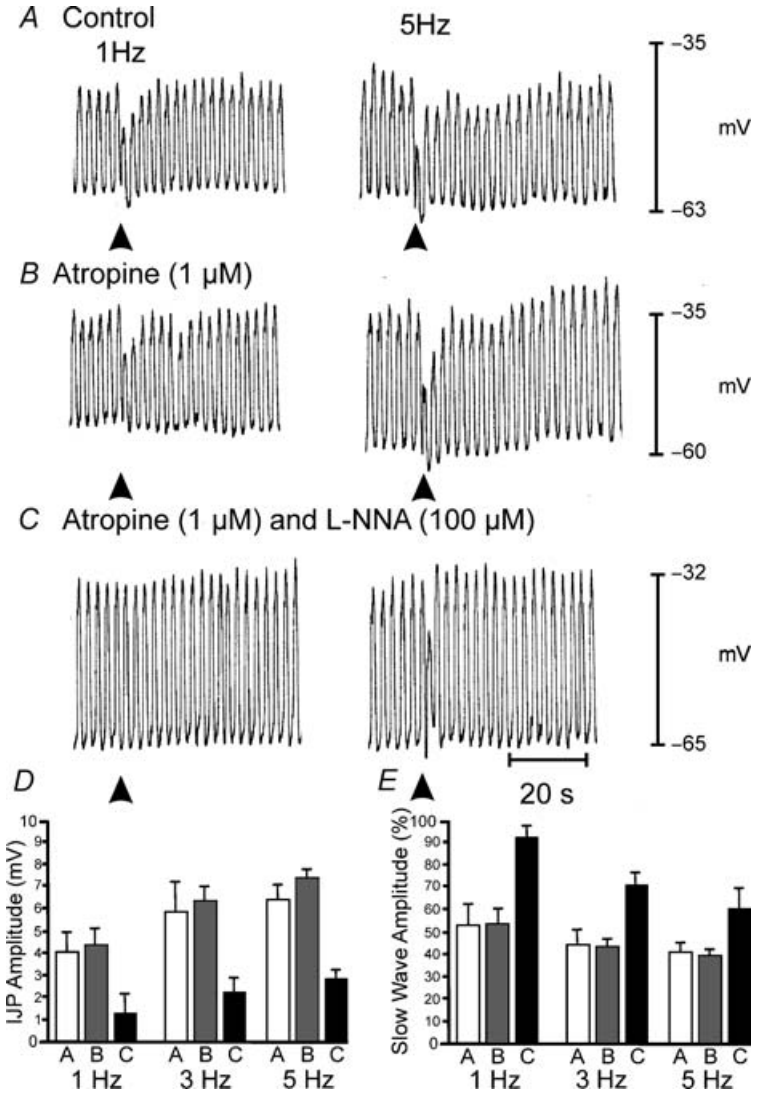

Figure 4. Neural responses in P10 animals after development of ICC-DMP
A, shows responses to EFS delivered at 1 and 5 Hz for 1 s (duration, 0.5 ms) indicated by arrowheads. Responses consisted of a reduction in the amplitude in the slow wave immediately following EFS and the development of a fast IJP. The IJP was followed by a reduction in the amplitude of slow waves for several cycles following EFS before returning to pre-stimulus levels. The reduction in the amplitude of slow waves was frequency dependent. *B*, atropine (1 μM) did not significantly increase the amplitude of the fast IJP but potentiated the reduction in the amplitude of the slow wave immediately following EFS and enhanced the reduction in slow-wave amplitude for 8–14 cycles following EFS at all frequencies. *C*, in the presence of atropine, L-NNA (200 μM) reduced the attenuation in slow-wave amplitude immediately following EFS and inhibited the IJP. L-NNA also blocked the reduction in slow-wave amplitude that occurred over several cycles after EFS. *D*, summarizes the effects of EFS on IJPs under control conditions (open bar), in the presence of atropine (1 μM, grey bars) and in the presence of atropine plus L-NNA (200 μM, filled bar) at 1, 3 and 5 Hz. *E*, summarizes the reduction in slow-wave amplitude following EFS as a percentage of the average amplitude of three slow waves immediately prior to EFS. Changes in slow-wave amplitude are shown under control conditions (open bar), in the presence of atropine (1 μM; grey bar) and in the presence of atropine plus L-NNA (200 μM; filled bar) at 1, 3 and 5 Hz.

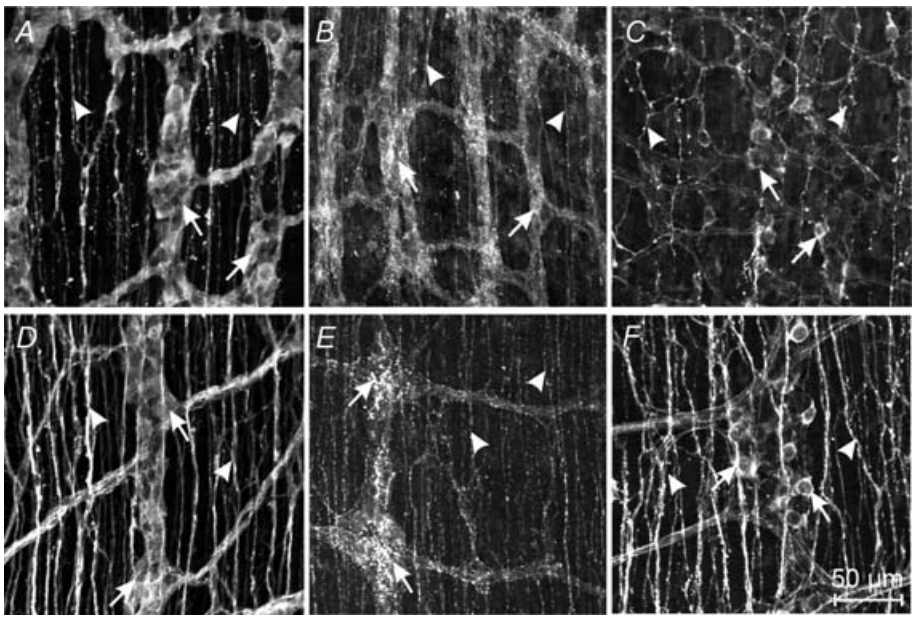

Figure 5. Enteric ganglia and neural processes in the circular muscle are present in the jejunum at P0 in mice
Expression of protein gene product 9.5 (PGP 9.5), vesicular acetylcholine transporter (vAChT) and neuronal nitric oxide synthase (nNOS) are shown by immunohistochemical techniques in tissues from P0 and P10 animals. *A–C*, PGP 9.5, vAChT-like and nNOS immunoreactvity is shown in neural cell bodies (arrows) and processes (arrowheads) in a P0 animal, respectively. *D–F*, show PGP 9.5, vAChT-like and nNOS immunoreactvity in cell bodies (arrows) and processes (arrowheads) from the deep muscular plexus of the circular muscle layer of a P10 jejunum, respectively. Note that vAChT primarily labels nerve processes and varicosities within the circular muscle layers. Scale bar in *F* applies to all panels.

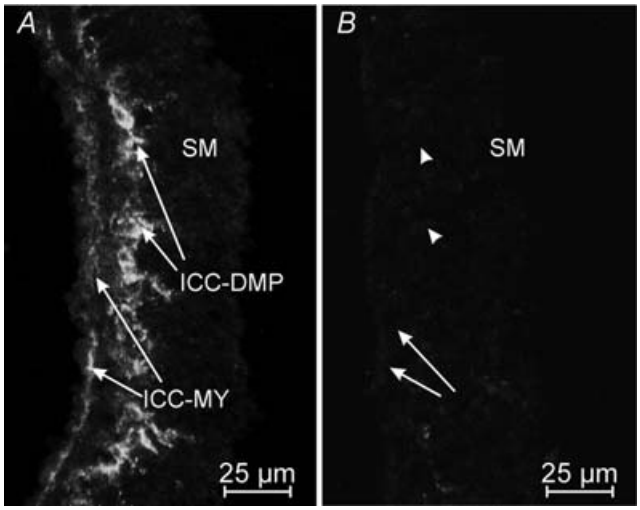

Figure 6. Culturing P0 tissues in the presence of Kit-neutralizing antibody for 7–9 days inhibited the expression of ICC-MY and ICC-DMP in jejunal tissues
A and *B*, are cryostat sections of jejunum from a P0 animal that were organ cultured for 8 days in the absence (*A*) and the presence (*B*) of the Kit-neutralizing antibody (ACK2; 5 μg ml^{-1}). Control tissues were also incubated with non-immune serum (data not shown). ICC-MY were maintained in organ culture and ICC-DMP developed over 7–9 days. In *B*, culturing tissues in the presence of ACK2 inhibited the maintenance of ICC-MY (arrows) and blocked the development of ICC-DMP (arrowheads). Scale bar is as indicated in each panel.

PGP 9.5, vAChT-like and nNOS-like immunoreactive nerve fibres (Fig. 5*D–F*, respectively) were readily apparent at the level of the deep muscular plexus. The density of nerve fibres was similar to that observed in adult tissues

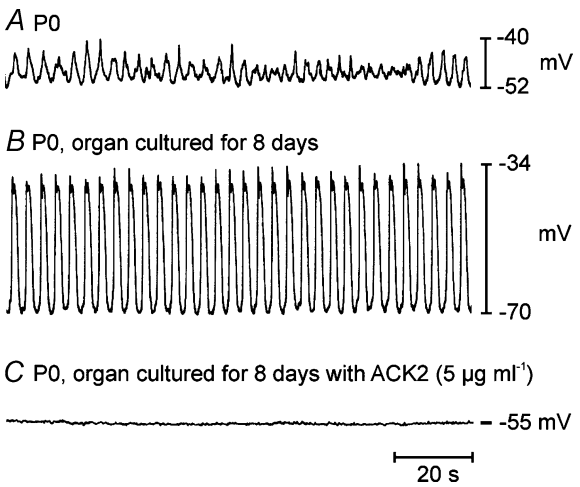

Figure 7. Electrical slow waves develop in organ culture and are inhibited by Kit-neutralizing antibody
A, shows slow-wave activity recorded from the jejunum of a P0 animal. Slow waves were small in amplitude and irregular in frequency. *B*, P0 jejunal tissues that were organ cultured for 8 days developed robust slow-wave activity similar to that observed *in vivo* (see Fig. 1). *C*, P0 jejunal tissues organ cultured for 8 days in the presence of ACK2 (5 μg ml^{-1}) had less-negative membrane potentials and no slow waves.

(P30; data not shown). It should be noted that vAChT antibodies mainly labelled varicose nerve fibres in P0 and P10 tissues.

Development of ICC-DMP and enteric inhibitory responses in organ cultures

Jejunal muscles cultured for 7–9 days from birth retained ICC-MY and developed an abundant population of Kit-positive cells at the level of the deep muscular plexus (Fig. 6*A*). Jejunal muscles cultured in the presence of Kit-neutralizing antibody (ACK2; 5 μl ml^{-1}) lost Kit-positive cells at the level of the myenteric and deep muscular plexuses ($n = 5$; Fig. 6*B*).

Jejunal muscles (Fig. 7*A*), cultured from P0 for 7–9 days, displayed slow-wave activity that was similar in amplitude but slower in frequency than the activity typically recorded from muscles of P10 animals. The mean resting membrane potential of cells in cultured muscles was -65 ± 1 mV ($n = 17$). Slow-wave amplitude averaged 29 ± 1 mV ($n = 81$), and slow-wave frequency averaged 18.4 ± 0.4 cycles min^{-1} ($n = 81$; Fig. 7*B*). There were no statistical differences in tissues that were cultured in M199 or with non-immune serum added ($P > 0.05$ for all parameters). In sharp contrast, tissues cultured for 7–9 days in the presence of neutralizing Kit antibody had less negative resting potentials, averaging -57 ± 1 mV ($n = 15$, $P < 0.001$), and slow waves were not recorded in these muscles (Fig. 7*C*).

EFS of cultured jejunal muscles (1–5 Hz for 1 s) resulted in small IJPs and reduction in slow-wave amplitude. Immediately after the stimulus, a depolarization rebound response occurred, upon which slow waves were superimposed (Fig. 8*A*). In some preparations, the initial IJP was masked by the upstroke of a slow wave. The small IJPs present under control conditions were enhanced by atropine (1 μM; Fig. 8*B*). Atropine did not affect the rebound excitation following IJPs. Subsequent addition of L-NNA (200 μM) reduced the amplitudes of IJPs (for example for EFS at 1 Hz, L-NNA reduced the amplitude of IJPs by 67% in six tissues; $P < 0.05$ compared to responses in the presence of atropine

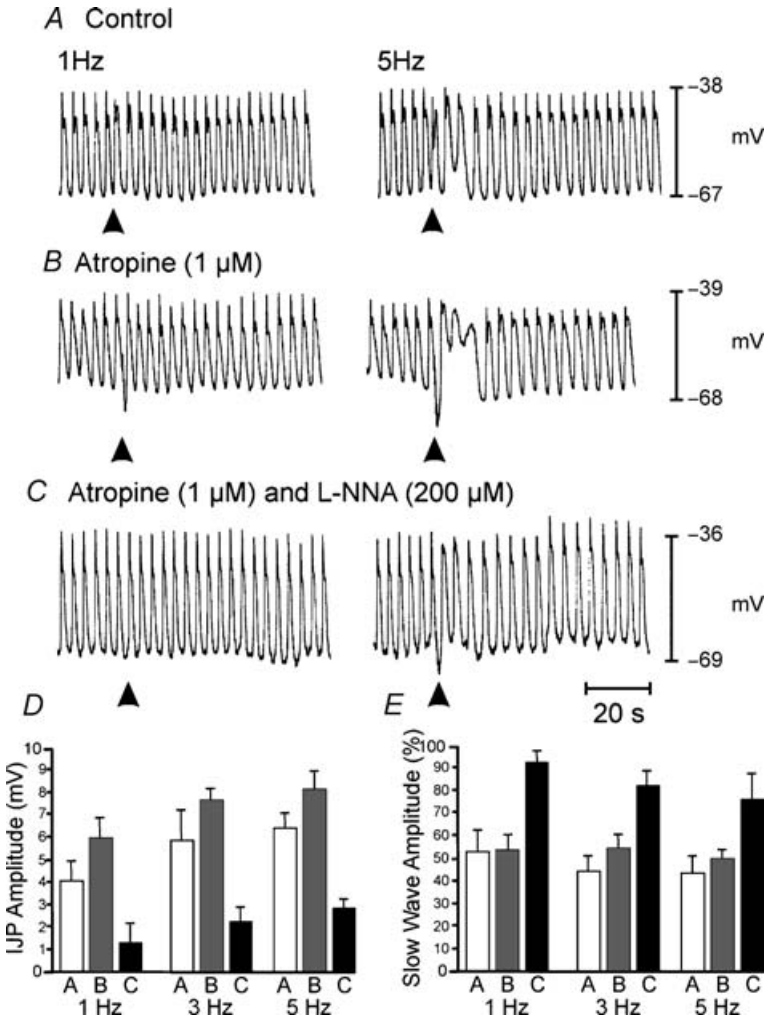

Figure 8. Normal post-junctional neural responses develop within 7–10 days in organ culture
A, shows neural responses to EFS at 1 and 5 Hz for 1 s (duration, 0.5 ms) under control conditions delivered at the arrow head. EFS produced attenuation of slow-wave amplitude. At frequencies of $\geq$ 3 Hz the inhibitory response was followed by an excitatory off response that caused, in some cases, summation of slow waves for 2–3 cycles. IJPs were prominent after addition of atropine (1 μM; *B*) and were followed by off responses. *C*, the addition of L-NNA (200 μM) in the presence of atropine abolished the IJP after one pulse and reduced IJP amplitudes at 5 Hz. Off responses in the presence of atropine plus L-NNA were still observed at 5 Hz but were reduced in amplitude. *D*, summarizes the IJP amplitude at 1, 3 and 5 Hz under control conditions (open bar), in the presence of atropine (1 μM; grey bar) and in the presence of atropine plus L-NNA (200 μM; filled bar). *E*, summarizes the slow-wave amplitude following EFS as a percentage of the average amplitude of three slow waves immediately prior to EFS. Changes in slow-wave amplitude are shown under control conditions (open bar), in the presence of atropine (1 μM; grey bar) and in the presence of atropine plus L-NNA (200 μM; filled bar) at 1, 3 and 5 Hz.

alone) and the reduction in slow-wave amplitude following EFS (Fig. 8*C*). The amplitudes of nerve-evoked responses increased with stimulation frequency (1–10 Hz). Preparations demonstrating IJPs at low frequencies (1–3 Hz) developed rebound responses at > 5 Hz which muted or masked the IJPs. Preparations in which IJPs were masked by depolarization did not show resolvable IJPs at any stimulation frequency. A summary of the neural responses of tissues maintained in organ culture is shown in Fig. 8*D* and *E*.

In muscles cultured with the Kit-neutralizing antibody, ACK2, EFS evoked primarily depolarization, which amounted to an off response ($n = 8$). In an additional four muscles, small fast IJPs were evoked at 1 Hz, but as stimulus frequency increased, IJPs were less common and observed in only 1 of 7 muscles stimulated at 10 Hz. The magnitude of the depolarization response was frequency dependent (Fig. 9*A*). In muscles cultured with ACK2, atropine (1 μM) did not affect the amplitude of the depolarization off response (Fig. 9*B*; $n = 8$, 1–10 Hz stimulation; $P > 0.05$). L-NNA (200 μM) did not affect the small fast IJPs observed in a few muscles (Fig. 9*C*; $n = 8$, 1–10 Hz; $P > 0.05$). In the presence of L-NNA plus atropine, the fast IJP was slightly, but not significantly, increased in amplitude by 30% and 49% at 1 and 5 Hz, respectively. The off responses were also not affected by L-NNA (Fig. 9*C*; $n = 8$, 1–10 Hz stimulation; $P > 0.05$). Thus, jejunal muscles lost significant responsiveness to cholinergic and nitrergic neural inputs after culturing with Kit-neutralizing antibody. Figure 9*D* summarizes the loss of neural responses in cultured muscles exposed to ACK2.

A possible explanation for the loss of enteric motor responses in muscles cultured with ACK2 could be that the antibody adversely affects neurons. To investigate this possibility we examined jejunal muscles cultured for 10 days with and without ACK2 using antibodies for the neuronal markers PGP 9.5, vAChT and nNOS. In control cultures, whole mounts labelled with PGP 9.5 revealed enteric neurons and a dense fibre network (Fig. 10*A*). Culturing appeared to reduce the overall organization of the myenteric plexus as compared to tissues removed from P10 animals (compare Fig. 5*D* with Fig. 10*A*). There was still an abundance of varicose fibres innervating the region of the deep muscular plexus after culturing for 10 days. Enteric excitatory and inhibitory neurons and processes were also visible in cultured muscles (Fig. 10*B* and *C*, respectively). Culturing with ACK2 had no affect on the pattern and distribution of neurons with PGP 9.5-, vAChT- and nNOS-like immunoreactivity (Fig. 10*D*–*F*, respectively).

Discussion

In the present study we investigated the development of post-junctional responses to EFS and the development of the network of ICC in the region of the deep muscular plexus (ICC-DMP) in the mouse. We used Kit immunoreactivity as a marker for ICC because previous studies employing electron microscopy and immunoelectron microscopy have demonstrated that Kit antibodies label mature and developing ICC in the mouse (Ward *et al.* 1994; Torihashi *et al.* 1995, 1997). At birth there was little or no neuromuscular regulation by cholinergic or nitrergic nerves in the circular muscle layer of the small intestine despite the presence of cholinergic and nitrergic immunopositive enteric neurons and nerve processes at the level of the deep muscular plexus. By P10, however, prominent cholinergic excitatory responses and nitrergic IJPs were recorded in response to EFS. Thus, during the first 10 days after birth, cholinergic excitatory and nitrergic inhibitory neurotransmission developed in murine jejunal muscles. The onset of neural responses corresponded with the development of ICC-DMP. Further studies were performed with Kit-neutralizing antibodies which blocked the development of ICC-DMP. In these

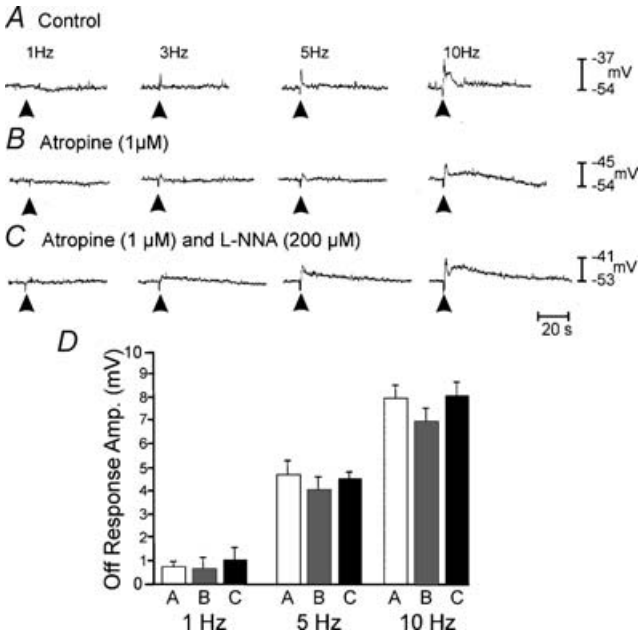

Figure 9. Jejunal tissues cultured in the presence of Kit-neutralizing antibody show reduced post-junctional neural responses

A, shows neural responses to EFS at 1–10 Hz for 1 s (duration, 0.5 ms) under control conditions delivered at the points indicated by the arrowheads. Neural responses consisting of off responses were only resolved at frequencies greater than 3 Hz. *B*, atropine (1 μM) did not affect the amplitude of responses to EFS, but there was an increase in the durations of off responses to 10 Hz after addition of atropine. *C*, in the continued presence of atropine, L-NNA (200 μM) had no significant effect on the nerve-evoked events. Downward deflections in the traces at the points of EFS represent stimulus artifacts. *D*, summarizes the amplitudes of the off responses under control conditions (A, open bar) in the presence of atropine (B; grey bar) and in the presence of atropine plus L-NNA (C, filled bar) at 1, 5 and 10 Hz.

muscles, cholinergic and nitrergic responses failed to develop in spite of innervation of the circular muscle layer. Together with previous data showing that excitatory and inhibitory motor nerve terminals are closely associated with ICC-DMP (see Wang *et al.* 1999; Iino *et al.* 2004), the present study supports the hypothesis that ICC-DMP, like intramuscular ICC in the stomach and oesophageal and pyloric sphincters (Burns *et al.* 1996; Ward *et al.* 1998, 2000), play a role in mediating cholinergic and nitrergic neurotransmission in the small bowel.

A developmental approach to investigate the role of ICC-DMP in neurotransmission was used in the present study. Neurons colonize the gut (Kapur *et al.* 1992; Pachnis *et al.* 1993; Young *et al.* 1998) and differentiate into functional classes, such as inhibitory and excitatory motor neurons (this study), before ICC-DMP develop (Torihashi *et al.* 1995). By embryonic day 14, neural precursors have colonized the entire length of the developing gut, and they develop into enteric neurons in a rostral to caudal manner (Young *et al.* 1999). Nitric oxide synthase-containing neurons develop prior to birth (Young *et al.* 1999). We confirmed this finding by showing that nitrergic and cholinergic neurons with processes extending into the circular muscle layer were present in the jejunum at birth. At P0, however, nitrergic and cholinergic post-junctional responses were not prominent. These responses emerged after the development of the ICC-DMP, suggesting an important role for these cells in mediating post-junctional neural responses.

ICC-DMP have been recognized as a cellular component in the deep muscular plexus for a number of years (see reviews by Thuneberg, 1982; Rumessen, 1994), but little about their function has been clearly established. A persistent finding of morphological studies has been that ICC-DMP lie in close association with varicose terminals of enteric motor neurons (e.g. Duchon *et al.* 1974; Yamamoto, 1977; Zhou & Komuro, 1992). More recent studies have documented the intimate and extensive relationship, including regions of synaptic specializations, between enteric motor neurons and ICC with confocal and immunoelectron microscopy in intestinal muscles of dog, guinea-pig, mouse and humans (Torihashi *et al.* 1993; Wang *et al.* 1999; Wang *et al.* 2000; Wang *et al.* 2003*b*). Evidence suggesting functional innervation of ICC-DMP has been provided by studies where stimulation of intrinsic nerves in isolated strips of murine small intestine caused atropine-sensitive translocation of protein kinase C and internalization of Neurokinin 1 receptors that are abundantly expressed on ICC-DMP (Wang *et al.* 2003*a*; Iino *et al.* 2004).

The apparent role of ICC-DMP in cholinergic and nitrergic neurotransmission suggests that specialized

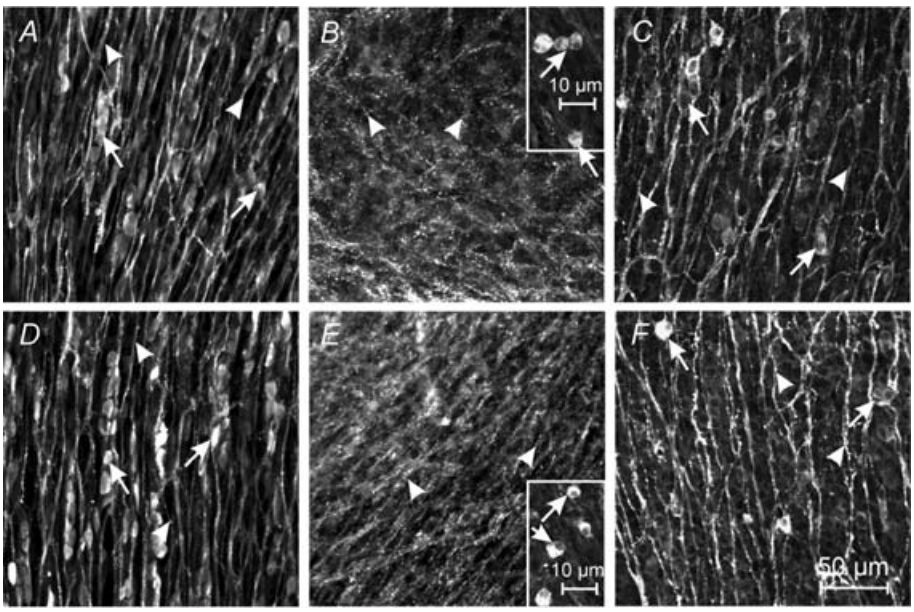

Figure 10. Enteric neurons and nerve fibres are present after culture with Kit-neutralizing antibody
Protein gene product 9.5 (PGP 9.5), vesicular acetylcholine transporter (vAChT) and neuronal nitric oxide synthase (nNOS) in P0 jejunal muscles cultured for 10 days in the absence and presence of Kit-neutralizing antibody. *A–C*, show PGP 9.5- (*A*), vAChT- (*B*) and nNOS- (*C*) immunopositive cell bodies (arrows) and nerve processes (arrowheads) in jejunal tissues from a P0 animal cultured for 10 days. *D–F*, show PGP 9.5 (*D*), vAChT-like (*E*) and nNOS (*F*) immunoreactvity in enteric neurons (arrows) and nerve fibres (arrowheads) from the deep muscular plexus of the circular layer of tissue cultured with ACK2 for 10 days. Note that vAChT primarily labels nerve processes and varicosities within the circular muscle layers but occasional cell bodies were also labelled (insets in *B* and *E*). Scale bar in *F* applies to all panels except insets in *B* and *E*.

receptors, second messenger systems and/or ionic conductances may be concentrated in these cells. It was reported previously that other ICC that are closely associated with motor neurons respond to nitrergic nerve stimulation and exogenous NO with increased levels of cGMP (see Shuttleworth *et al.* 1993; Young *et al.* 1993), and cGMP-dependent protein kinase and soluble guanylyl cyclase have been reported to be expressed in ICC-DMP in the rat small intestine (Huber *et al.* 1998; Salmhofer *et al.* 2001). Studies have not yet determined the responses of ICC-DMP to neurotransmitters because it has not been possible to identify ICC-DMP in fresh enzymatic cell dispersions of the muscularis.

The results of the present study confirm previous observations that ICC-MY and ICC-DMP develop at different times. Others have reported that ICC-MY networks are incomplete and slow waves are not present in neonatal animals (Liu *et al.* 1998). These authors, using methylene blue as a marker for ICC, concluded that ICC-MY networks develop mainly after birth. That conclusion is in stark contrast to the observations in the present study in which Kit labelling clearly demonstrated the presence of well-formed ICC-MY networks at birth in murine jejunum. ICC-DMP were not observed in ileal muscles at birth in a previous study (Torihashi *et al.* 1997), but a small, scattered population of ICC-DMP was observed in whole-mount preparations in the present series of experiments. Thus, a gradient in the timing of development of ICC-DMP may exist along the small intestine, as has been noted in the development of ICC-MY (Ward *et al.* 1997). Our data suggest that a similar sequence may occur in the development of cholinergic and nitrergic innervation; however, specific studies to closely follow the time course of development of post-junctional responses were not performed.

In summary, developmental studies in which nitrergic and cholinergic responses were evaluated before and after development of ICC-DMP networks, and in tissues in which neutralizing Kit antibodies were used to block the development of ICC-DMP, suggest that this class of ICC is an important mediator of enteric motor neurotransmission. These findings suggest that ICC-DMP are functionally similar to other ICC located within muscle layers (ICC-IM) that also form close associations with enteric motor neurons. Unlike ICC-IM in the stomach, however, which appear to be relatively evenly distributed throughout the circular and longitudinal muscle layers (see Burns *et al.* 1996), ICC-DMP lie in a specific plane of the circular muscle layer that is heavily innervated by enteric motor neurons. The functional reasons for the differences in neural and ICC architecture in the small bowel and stomach, and the developmental factors responsible for alignment of ICC and nerve terminals in a specific plane within the small intestine, are still to be determined. Innervation of GI muscles does not appear to be essential for the development of ICC, as normal ICC were observed in Glial cell line-derived neurotrophic factor (GDNF) knock-out mice, which lack enteric nerves below the gastric fundus (Ward *et al.* 1999). The opposite is also true because normal-appearing enteric motor nerve fibres and terminals are found in the tissues of animals lacking ICC-IM (Burns *et al.* 1996; Ward *et al.* 2000). It is clear, however, that nerves innervating the muscle layers of the gut find and form close, functional associations with ICC-IM and ICC-DMP. Thus damage or loss of these cells, as observed in type 1 diabetes (Ordog *et al.* 2000), in a region of bowel proximal to an intestinal obstruction (Chang *et al.* 2001), or following intestinal resection (Yanagida *et al.* 2004), could cause or contribute to GI motor dysfunction that gastroenterologists have attributed to neuropathies in the past.

References

Beckett EAH, McGeough CA, Sanders KM & Ward SM (2003). Pacing of interstitial cells of Cajal in the murine gastric antrum: neurally mediated and direct stimulation. *J Physiol* **553**, 545–559.

Burns AJ, Lomax AEJ, Torihashi S, Sanders KM & Ward SM (1996). Interstitial cells of Cajal mediate inhibitory neurotransmission in the stomach. *Proc Natl Acad Sci U S A* **93**, 12008–12013.

Chang I-Y, Glasgow NJ, Takayama I, Horiguchi K, Sanders KM & Ward SM (2001). Loss of interstitial cells of Cajal and development of electrical dysfunction in murine small bowel obstruction. *J Physiol* **536**, 555–568.

Dickens EJ, Hirst GD & Tomita T (1999). Identification of rhythmically active cells in guinea-pig stomach. *J Physiol* **514**, 515–531.

Duchon G, Henderson R & Daniel EE (1974). Circular muscle layers in the small intestine. *Proceedings of the 4th International Symposium on Gastrointestinal Motility*. Banff, Alberta, Canada, pp. 635–646.

Hirst GDS, Beckett EAH, Sanders KM & Ward SM (2002). Regional variation in contribution of myenteric and intramuscular interstitial cells of Cajal to generation of slow waves in mouse gastric antrum. *J Physiol* **540**, 1003–1012.

Huber A, Trudrung P, Storr M, Franck H, Schusdziarra V, Ruth P & Allescher HD (1998). Protein kinase G expression in the small intestine and functional importance for smooth muscle relaxation. *Am J Physiol* **275**, G629–G637.

Huizinga JD, Thuneberg L, Kluppel M, Malysz J, Mikkelsen HB & Bernstein A (1995). W/kit gene required for intestinal pacemaker activity. *Nature* **373**, 347–349.

Iino S, Ward SM & Sanders KM (2004). Interstitial cells of Cajal are functionally innervated by excitatory motor neurons in the murine intestine. *J Physiol* **556**, 521–530.

Kapur RP, Yost C & Palmiter RD (1992). A transgenic model for studying development of the enteric nervous system in normal and aganglionic mice. *Development* **116**, 167–175.

Langton P, Ward SM, Carl A, Norell MA & Sanders KM (1989). Spontaneous electrical activity of interstitial cells of Cajal isolated from canine proximal colon. *Proc Natl Acad Sci U S A* **86**, 7280–7284.

Lavin ST, Southwell BR, Murphy R, Jenkinson KM & Furness JB (1998). Activation of neurokinin 1 receptors on interstitial cells of Cajal of the guinea-pig small intestine by substance P. *Histochem Cell Biol* **110**, 263–271.

Liu LW, Thuneberg L & Huizinga JD (1998). Development of pacemaker activity and interstitial cells of Cajal in the neonatal mouse small intestine. *Dev Dyn* **213**, 271–282.

Maeda H, Yamagata A, Nishikawa S, Yoshinaga K, Kobayashi S, Nishi K & Nishikawa S (1992). Requirement of c-*kit* for development of intestinal pacemaker system. *Development* **116**, 369–375.

Nocka K, Tan JC, Chiu E, Chu TY, Ray P, Traktman P & Besmer P (1990). Molecular bases of dominant negative and loss of function mutations at the murine c-kit/white spotting locus: W37, Wv, W41 and W. *EMBO J* **9**, 1805–1813.

Ordog T, Takayama I, Cheung WK, Ward SM & Sanders KM (2000). Remodeling of networks of interstitial cells of Cajal in a murine model of diabetic gastroparesis. *Diabetes* **49**, 1731–1739.

Pachnis V, Mankoo B & Costantini F (1993). Expression of the c-ret proto-oncogene during mouse embryogenesis. *Development* **119**, 1005–1117.

Rumessen JJ (1994). Identification of interstitial cells of Cajal. Significance for studies of human small intestine and colon. *Dan Med Bull* **41**, 275–293.

Salmhofer H, Neuhuber WL, Ruth P, Huber A, Russwurm M & Allescher HD (2001). Pivotal role of the interstitial cells of Cajal in the nitric oxide signaling pathway of rat small intestine. Morphological evidence. *Cell Tissue Res* **305**, 331–340.

Sanders KM (1996). A case for interstitial cells of Cajal as pacemakers and mediators of neurotransmission in the gastrointestinal tract. *Gastroenterology* **111**, 492–515.

Shuttleworth CW, Xue C, Ward SM, de Vente J & Sanders KM (1993). Immunohistochemical localization of 3′,5′-cyclic guanosine monophosphate in the canine proximal colon: responses to nitric oxide and electrical stimulation of enteric inhibitory neurons. *Neuroscience* **56**, 513–522.

Suzuki H, Ward SM, Bayguinov YR, Edwards F & Hirst GDS (2003). Involvement in intramuscular interstitial cells of Cajal in nitrergic inhibition in the mouse gastric antrum. *J Physiol* **546**, 751–763.

Thuneberg L (1982). Interstitial cells of Cajal: intestinal pacemakers? *Adv Anat Embryol Cell Biol* **71**, 1–130.

Torihashi S, Kobayashi S & Sanders KM (1993). Interstitial cells in deep muscular plexus of canine small intestine may be specialized smooth muscle cells. *Am J Physiol* **265**, G638–G645.

Torihashi S, Ward SM, Nishikawa S-I, Nishi K, Kobayashi S & Sanders KM (1995). c-*kit*-dependent development of interstitial cells and electrical activity in the murine gastrointestinal tract. *Cell Tissue Res* **280**, 97–111.

Torihashi S, Ward SM & Sanders KM (1997). Development of c-Kit-positive cells and the onset of electrical rhythmicity in murine small intestine. *Gastroenterology* **112**, 144–155.

Wang XY, Paterson C & Huizinga JD (2003*b*). Cholinergic and nitrergic innervation of ICC-DMP and ICC-IM in the human small intestine. *Neurogastroenterol Motil* **15**, 531–543.

Wang XY, Sanders KM & Ward SM (1999). Intimate relationship between interstitial cells of Cajal and enteric nerves in the guinea-pig small intestine. *Cell Tissue Res* **295**, 247–256.

Wang XY, Sanders KM & Ward SM (2000). Relationship between interstitial cells of Cajal and enteric motor neurons in the murine proximal colon. *Cell Tissue Res* **302**, 331–342.

Wang XY, Ward SM, Gerthoffer WT & Sanders KM (2003*a*). Protein kinase Cε translocation in enteric neurons and interstitial cells of Cajal in response to muscarinic stimulation. *Am J Physiol Gastrointest Liver Physiol* **285**, G593–G601.

Ward SM, Beckett EAH, Wang X-Y, Baker F, Khoyi M & Sanders KM (2000). Interstitial cells of Cajal mediate cholinergic neurotransmission from enteric motor neurons. *J Neurosci* **20**, 1393–1403.

Ward SM, Burns AJ, Torihashi S, Harney SC & Sanders KM (1995). Impaired development of interstitial cells and intestinal electrical rhythmicity in *steel* mutants. *Am J Physiol* **269**, C1577–C1585.

Ward SM, Burns AJ, Torihashi S & Sanders KM (1994). Mutation of the proto-oncogene c-*kit* blocks development of interstitial cells and electrical rhythmicity in murine intestine. *J Physiol* **480**, 91–97.

Ward SM, Harney SH, Bayguinov JR, McLaren GJ & Sanders KM (1997). Development of electrical rhythmicity in the murine gastrointestinal tract is specifically encoded in the *tunica muscularis*. *J Physiol* **505**, 241–258.

Ward SM, Morris G, Reese L, Wang X-Y & Sanders KM (1998). Interstitial cells of Cajal mediate enteric inhibitory neurotransmission in the lower esophageal and pyloric sphincters. *Gastroenterology* **115**, 314–329.

Ward SM, Ordog T, Bayguinov JR, Horowitz B, Epperson A, Shen L, Westphal H & Sanders KM (1999). Development of interstitial cells of Cajal and pacemaking in mice lacking enteric nerves. *Gastroenterology* **117**, 584–594.

Won KJ, Sanders KM & Ward SM (2005). Interstitial cells of Cajal mediate mechanosensitive responses in the stomach. *Proc Natl Acad Sci U S A* **102**, 14913–14918.

Yamamoto M (1977). Electron microscopic studies on the innervation of the smooth muscle and the interstitial cell of Cajal in the small intestine of the mouse and bat. *Arch Histol Jpn* **40**, 171–201.

Yanagida H, Yanase H, Sanders KM & Ward SM (2004). Intestinal surgical resection disrupts electrical rhythmicity neural responses and ICC networks. *Gastroenterology* **127**, 1748–1759.

Young HM, Ciampoli D, Hsuan J & Canty AJ (1999). Expression of Ret-, p75 (NTR)-, Phox2a-, Phox2b-, and tyrosine hydroxylase-immunoreactivity by undifferentiated neural crest-derived cells and different classes of enteric neurons in the embryonic mouse gut. *Dev Dyn* **216**, 137–152.

Young HM, Hearn CJ, Ciampoli D, Southwell BR, Brunet JF & Newgreen DF (1998). A single rostrocaudal colonization of the rodent intestine by enteric neuron precursors is revealed by the expression of Phox2b, Ret, and p75 and by explants grown under the kidney capsule or in organ culture. *Dev Biol* **202**, 67–84.

Young HM, Jones BR & McKeown SJ (2002). The projections of early enteric neurons are influenced by the direction of neural crest cell migration. *J Neurosci* **22**, 6005–6018.

Young HM, McConalogue K, Furness JB & de Vente J (1993). Nitric oxide targets in the guinea-pig intestine identified by induction of cyclic GMP immunoreactivity. *Neuroscience* **55**, 583–596.

Zhou DS & Komuro T (1992). The cellular network of interstitial cells associated with the deep muscular plexus of the guinea pig small intestine. *Anat Embryol (Berl)* **186**, 519–527.

Acknowledgements

This project was supported by a research grant from the National Institute of Diabetics and Digestive and Kidney Diseases (NIDDK), DK41315. The authors are grateful to Julia Bayguinov and Nancy Horowitz for technical assistance. We are also grateful to Piers Emson from the Molecular Science Group, Cambridge, UK for the gift of nNOS antibody.